Supporting information for:

A Thermodynamic Description of the Adsorption of Simple Water-Soluble Peptoids to Silica

Anna C. Calkins, Jennifer Yin, Jacenda L. Rangel, Madeleine R. Landry, Amelia A. Fuller, Grace Y. Stokes*

Department of Chemistry and Biochemistry, Santa Clara University, 500 El Camino Real, Santa Clara, CA 95053

Table of Contents

1. Detailed SHG experimental procedures

a. SHG setup: The 532 nm laser light was directed through a λ/2 waveplate (#WPH10M-532, Thorlabs) and cube polarizer (#PBS12-532-HP) to adjust the power followed by a Galilean telescope (+100.0 mm plano-convex lens and -50.0 mm concave lens) to collimate and resize the beam to a final width of 3 mm. SHG signal was detected from the front face of the prism and passed through two filters: one 266 MaxLine© laser-line filter (Semrock, LL01-266) and one 260 nm/15 nm BrightLine© single-band bandpass filter (Semrock, FF01-260) into a photomultiplier tube (Hamamatsu R7154). The signal was processed with a gated integrator and boxcar average (Stanford Research Systems, SR250).

b. Flow cell description: Trapezoid-shaped fused silica (SiO_2) prisms were purchased from Almaz Optics (material = KU-1, UV-grade SiO_2) and polished on all sides that laser light passed through or was detected through. The flow cell body was composed of the chemically resistant polymer, polychlorotrifluoroethylene (PCTFE or Kel-F). Inlet and outlet ports utilized connectors and cap adapters made of polytetrafluoroethylene (PTFE), ferrules made of ethyltetrafluoroethylene (ETFE) and tubing made of tetrafluoroethylene (TFE). Teflon o-rings (Hydrapak, #2-015V/TE) were pressed between the SiO_2 prism and the CTFE flow cell to ensure a water-tight seal.

c. Normalization procedures: SHG intensities were corrected for changes in collection efficiency and day-to-day laser fluctuations using a two-point normalization procedure. At the end of each isotherm experiment, the SHG signal intensity at the solid-aqueous interface was recorded for a 0.01 M potassium hydroxide solution and PBS buffer (pH 7.4). SHG signal intensity varied with polarization of the incident laser light. We recorded counter-propagating

SHG polarization-dependent anisotropy curves for peptoids adsorbed to bare SiO_2 over 6 minutes of exposure to the laser at increasing peptoid concentrations to ensure the origin of the achiral second harmonic emission. Representative SHG anisotropy data for low versus high surface coverage of **1** and **2** are shown in Figure S1.

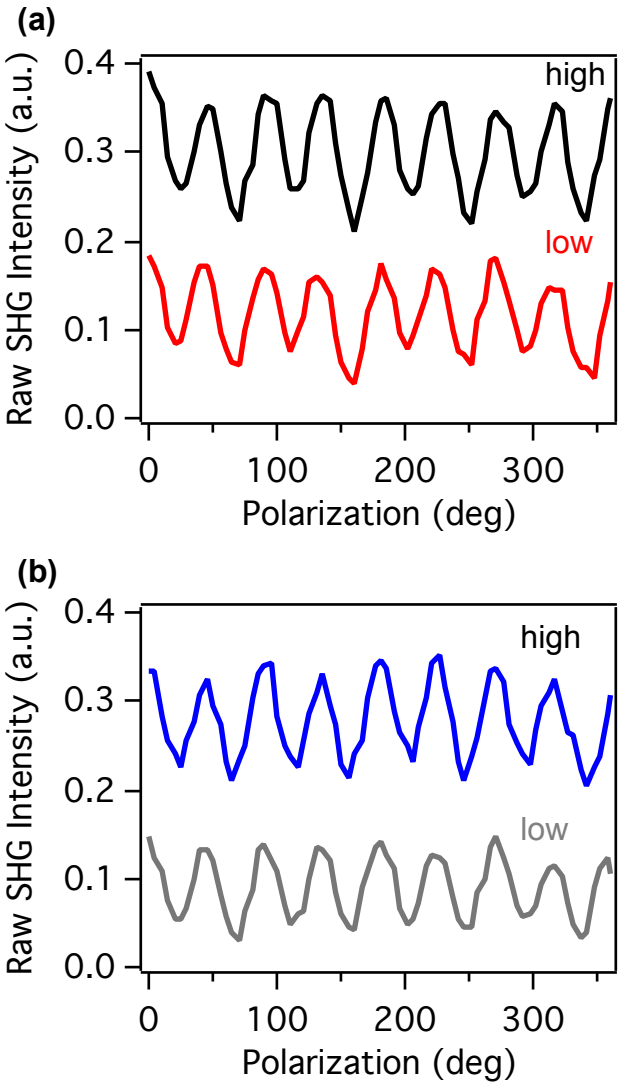

Figure S1. Representative polarization-dependent SHG anisotropy data for low ($1.0x10^{-6}$ M, red) and high ($4.0x10^{-5}$ M, black) concentrations of **1 (a)** and **2 (b)** adsorbed to SiO_2 in PBS buffer pH 7.4. Curves are offset for clarity.

2. Comparisons to proteins and small molecules

Table S1. Relevant charge, pI, molecular weight (MW), and K_a values from Langmuir fits reported for adsorption of small molecules, peptoids and proteins to SiO_2.

charge	pI	adsorbate	MW (g/mol)	K_a (M^{-1})	Analytical method
0	>9	1,1'-bi-2-naphthol	286	$2.6x10^5$	SHG[1]
+	>12	morantel citrate	412	$2.3x10^7$	SHG[2]
-	5	oxytetracycline hydrochloride	497	$1.3x10^5$	SHG[3]
+	>9	6-mer	898	$6.5\pm1.2\ x10^5$	SHG (this work)
+	>9	15-mer	2220	$3.4\pm0.8\ x10^6$	SHG (this work)
+	9.6	cytochrome c	12384	$8.2\ x10^6$	SHG[4a]
+	11.35	lysozyme	14331	$2.3\pm0.8\ x10^6$	CD spectroscopy[5]
-	4.7	bovine serum albumin	66463	$2.6\pm1.1\ x10^4$	Fluorometric assay[6]
-	4.4	bovine fibrinogen	340000	$2.37\pm0.48\ x10^5$	Fluorometric assay[6]

[a]cytochrome c data was extrapolated from the reported $\Delta_{ads}G$ = -11.8 kcal/mol

3. Derivation of simplified form of the Langmuir model (equation 5 in main text)

In Equation 1 in the main text, the nonresonant component contribution to the second-order susceptibility tensor, $\chi_{NR}^{(2)}$, is a real number as the buffer and SiO_2 do not exhibit electronic resonances at 266 nm. In contrast, the resonant contribution, $\chi_R^{(2)}$, is a complex number because SHG signal is resonant with the electronic transitions of **1** and **2**. Equation 1 from the main text can be re-written in the form below where we represent $\chi_{NR}^{(2)}$ as real number, a, and $\chi_R^{(2)}$ as complex number, $b+ic$.

$$I_{SHG} \propto \left|\chi_{NR}^{(2)} + \chi_R^{(2)}\right|^2 \propto \left|a + N(b+ic)\right|^2 \propto (a+Nb)^2 + (Nc)^2 \qquad \text{(S1)}$$

In equation S1, a is the non-resonant response from the background while b and ic are the real and imaginary components, respectively, of the resonant susceptibility due to adsorbed peptoid.

If we model the adsorption of **1** and **2** to SiO_2 with the Langmuir model, the surface density N in equation S1 is given by

$$N = \frac{N_{\max} K_a [peptoid]}{1 + K_a [peptoid]} \tag{S2}$$

In equation S2, N_{max} is the surface density at saturation, K_a is the equilibrium association constant, *[peptoid]* is the bulk peptoid concentration. Substitution of equation S2 into equation S1 results in the following relationship between measured SHG signal, N_{max}, K_a, and [*peptoid*].

$$I_{SHG} \propto \left(a + b \frac{N_{\max} K_a [peptoid]}{1 + K_a [peptoid]} \right)^2 + \left(c \frac{N_{\max} K_a [peptoid]}{1 + K_a [peptoid]} \right)^2$$

$$\propto a^2 + 2ab \frac{N_{\max} K_a [peptoid]}{1 + K_a [peptoid]} + (b^2 + c^2) \left(\frac{N_{\max} K_a [peptoid]}{1 + K_a [peptoid]} \right)^2 \tag{S3}$$

The SHG intensity due to the non-resonant background in the absence of peptoid is given by equation S4.

$$I_{SHG}^{background} \propto a^2 \tag{S4}$$

If we subtract the background contribution (equation S4) from the measured SHG signal (equation S3), we are left with the equation shown below.

$$I_{SHG} - I_{SHG}^{background} \propto 2ab \frac{N_{\max} K_a [peptoid]}{1 + K_a [peptoid]} + (b^2 + c^2) \left(\frac{N_{\max} K_a [peptoid]}{1 + K_a [peptoid]} \right)^2 \tag{S5}$$

To obtain the SHG intensity, which changes when peptoid adsorbs, we use the relationships given in the main text between surface density and SHG intensity (equations 1 and 2), plus the relationship between I_{SHG} and N^2 (equation 3) to obtain the equation below.

$$I_{SHG} - I_{SHG}^{background} \propto 2\sqrt{I_{SHG}^{background}}\, b \frac{\sqrt{I_{SHG}^{\max}} K_a[peptoid]}{1+K_a[peptoid]} + (b^2+c^2)\left(\frac{\sqrt{I_{SHG}^{\max}} K_a[peptoid]}{1+K_a[peptoid]}\right)^2 \quad \text{(S6)}$$

Note that $\sqrt{I_{SHG}^{\max}}$ is the square root of the maximum SHG intensity at surface saturation. To obtain the simplified form of the Langmuir model given in the main text, we made the assumption that the non-resonant SHG signal intensity can be considered negligible compared to the resonant contribution to eliminate the cross-term ($2\sqrt{I_{SHG}^{background}}\, b \frac{\sqrt{I_{SHG}^{\max}} K_a[peptoid]}{1+K_a[peptoid]}$) in equation S6. What we have left is equation S7 below, which is equivalent to equation 5 in the main text.

$$I_{SHG} \propto \left(\frac{\sqrt{I_{SHG}^{\max}} K_a[peptoid]}{1+K_a[peptoid]}\right)^2 \quad \text{(S7)}$$

$$I_{SHG} \propto \frac{\left(\max I_{SHG}\right) K_a^2[peptoid]^2}{\left(1+K_a[peptoid]\right)^2} \quad \text{(5)}$$

4. Adsorption of 2 to SiO_2 at concentrations above 10^{-5} M

The simplified Langmuir model (equation 5) was applied to the SHG intensities observed at concentrations ranging from $5x10^{-7}$ M to $4x10^{-5}$ M. The large errors associated with the dotted fit line (Figure S2) indicate that at high aqueous concentrations, adsorption of **2** deviates from simple Langmuir behavior. The Langmuir fit coefficients for the data shown below are equal to $K_a = 9.9\pm0.3\ x10^5\ M^{-1}$ and $maxI_{SHG} = 0.17\pm0.01$.

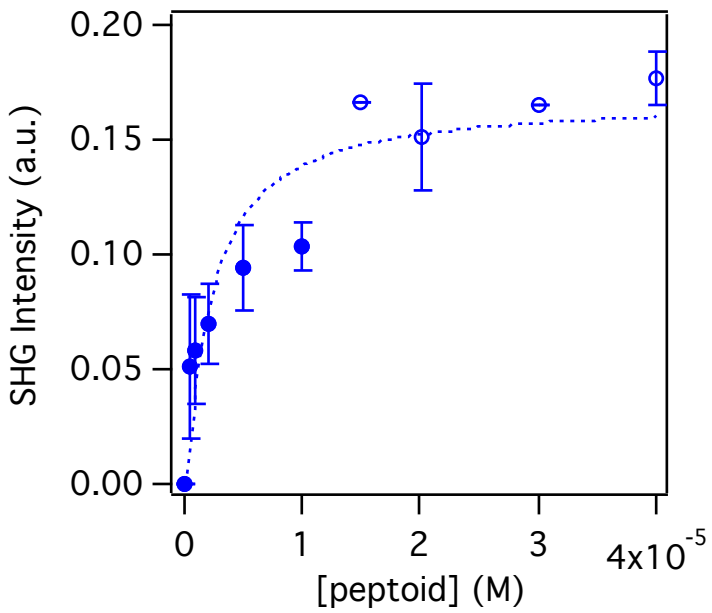

Figure S2. Adsorption isotherm of peptoid **2** fit to the Langmuir model (dotted line). Open circles correspond to SHG intensities at high aqueous concentrations that were not included in the Langmuir fits reported in the main text.

5. Desorption studies

To determine whether adsorption of peptoids is reversible, PBS buffer was flowed across a SiO_2 surface containing adsorbed peptoids **1** or **2**, and square root of SHG signal change was monitored (Figure S3). After 15 rinse cycles (1 cycle = 10 mL injection of PBS buffer plus 5 minute wait time), the SHG signal intensity due to **1** or **2** did not return to the initial signal intensity level observed in the absence of peptoid.

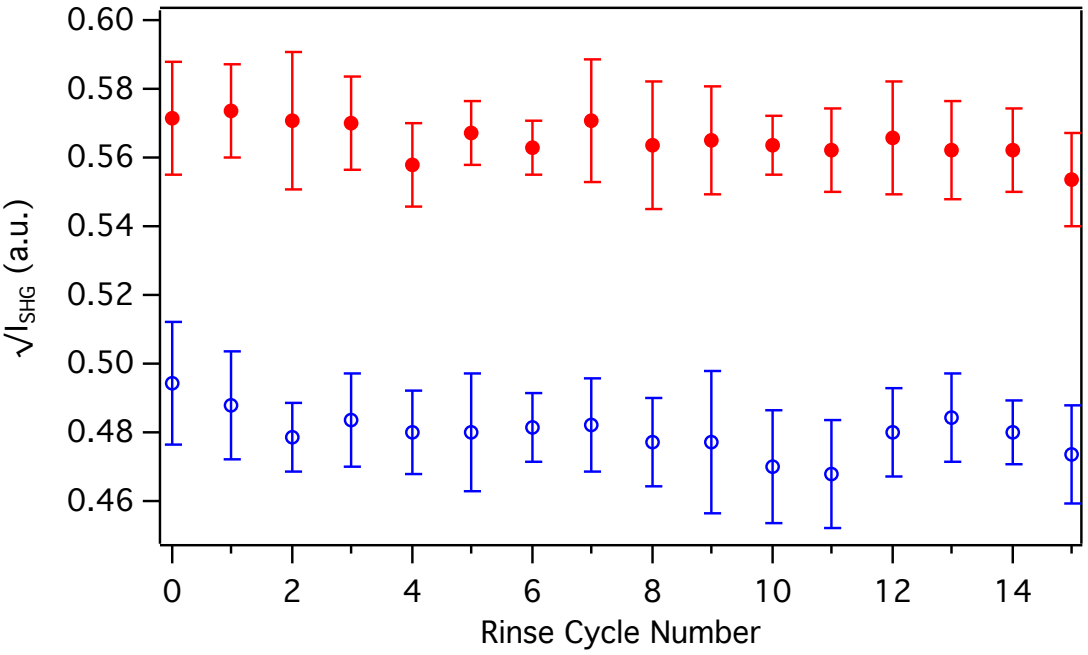

Figure S3. Square root of SHG intensities of **1** (top, red filled circles) and **2** (bottom, blue open circles) monitored after each rinse cycle (injection of 10 mL PBS buffer plus 5 minute waiting period). Data are offset for clarity.

6. Dynamic Light Scattering (DLS) studies

Nonporous SiO_2 microspheres used for fluorescence and circular dichroism (CD) experiments were purchased from Polysciences in two sizes, with diameters of 500 nm (#24323) and 50 nm (#24040), respectively. DLS measurements were conducted using a 90Plus Particle Size Analyzer (Brookhaven Instruments Corp) to confirm sizes and polydispersities reported by the manufacturer (Table S2). For fluorescence studies, which required quantitative analysis, SiO_2 spheres with larger diameter (500 nm) were used because of their more monodisperse sizes. For CD studies, which only required qualitative analysis, 50 nm spheres were used to minimize colloidal scattering of near-UV light. SiO_2 microspheres used in fluorescence studies were suspended in PBS buffer pH 7.4. CD studies utilized 50 mM phosphate buffer pH 7.4 (no NaCl).

Table S2. Size and polydispersity of SiO_2 microspheres measured by DLS

Polysciences (part #)	Reported size (nm)	DLS size (nm)	Surface area from DLS data (m^2/g)	Measured polydispersity index
24323	500±70	655 ± 13	4.6± 0.1	0.02 ± 0.15
24040	50±10	79 ± 6	38± 3	0.005 ± 0.008

7. Fluorescence spectroscopy

The calibration standards generated from these data indicate that fluorescence intensity at 337 nm or 392 nm for peptoids **1** and **2**, respectively, varies in a linear fashion with bulk peptoid concentration within this concentration range (Figure S4). Following equilibration with SiO_2 microspheres, the supernatant solution exhibits a decrease in the fluorescence intensity of **1** and **2**, which is attributed to the removal of peptoid adsorbed to SiO_2 microspheres (Figure S5). The depletion of fluorescence intensity following equilibration with 500 nm microspheres was used to indirectly determine concentrations of adsorbed peptoid.

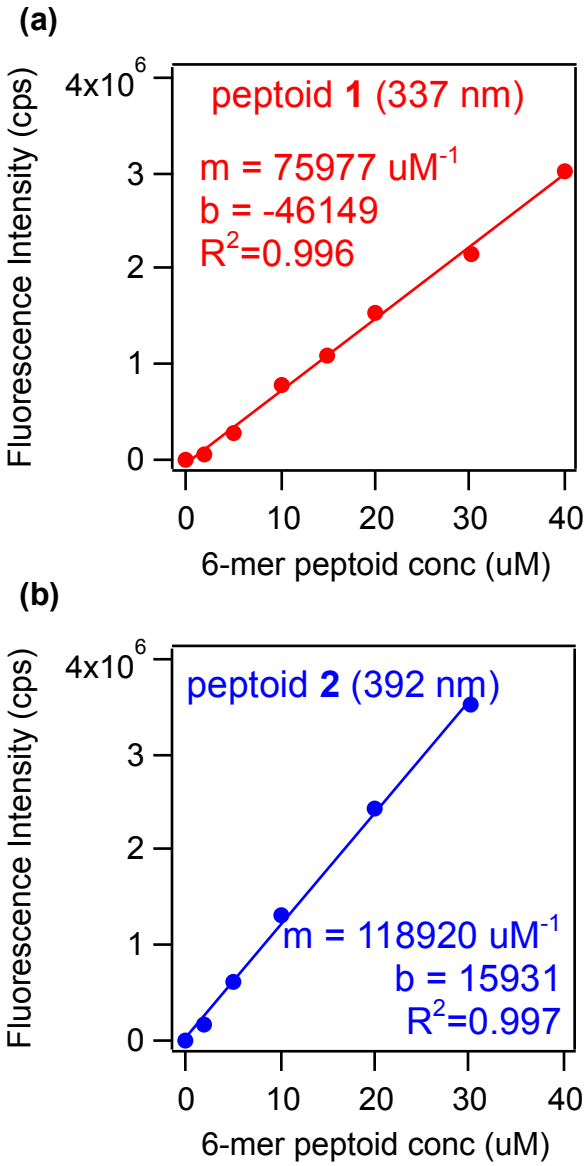

Figure S4. Fluorescence intensities for standard concentrations of peptoids **1** (**a**) and **2** (**b**), detected at emission wavelengths of 337 nm and 392 nm, respectively. Linear (y=mx+b) fit coefficients and R^2 errors are shown.

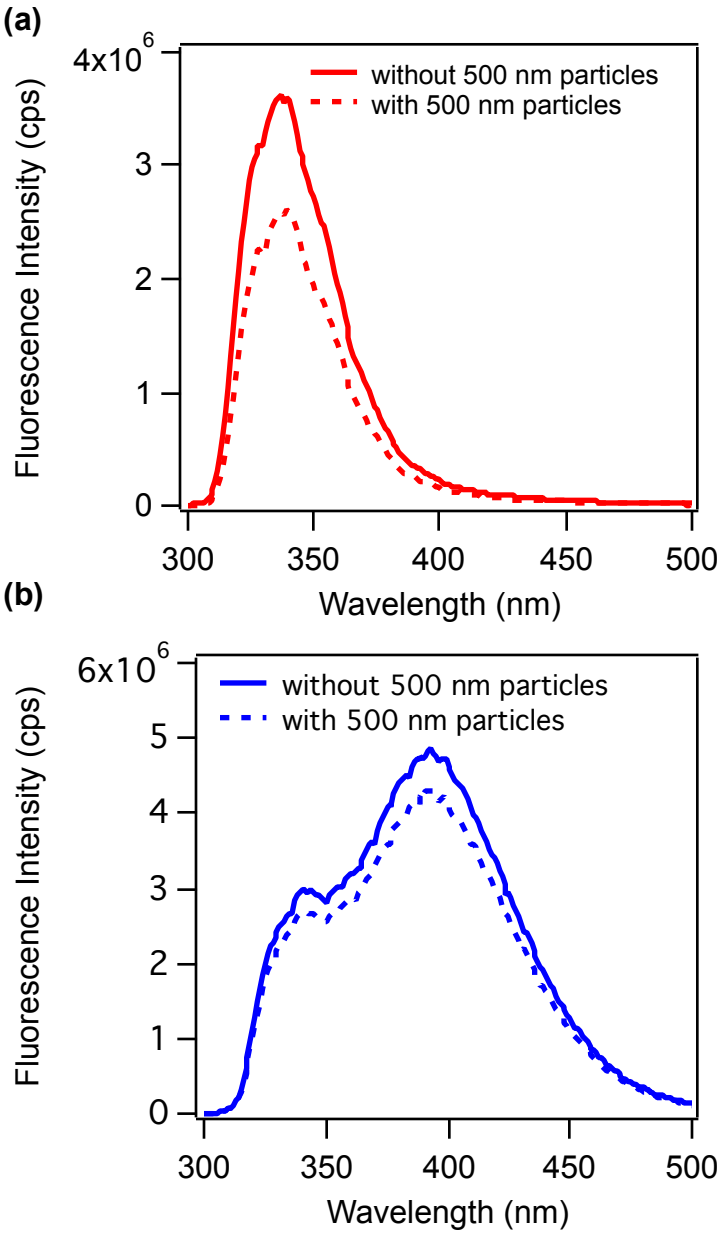

Figure S5. Fluorescence spectra for **1** (**a**) and **2** (**b**) observed in the supernatant after exposure to 5 g/L silica microspheres followed by removal by centrifugation (dashed line) and in the absence of microspheres (solid line).

8. References

(1) Petralli-Mallow, T.; Wong, T. M.; Byers, J. D.; Yee, H. I.; Hicks, J. M. Circular dichroism spectroscopy at interfaces: a surface second harmonic generation study. *J. Phys. Chem* **1993**, *97*, 1383-1388.

(2) Konek, C. T.; Illg, K. D.; Al-Abadleh, H. A.; Voges, A. B.; Yin, G.; Musorrafiti, M. J.; Schmidt, C. M.; Geiger, F. M. Nonlinear Optical Studies of the Agricultural Antibiotic Morantel Interacting with Silica/Water Interfaces. *J. Am. Chem. Soc.* **2005**, *127*, 15771-15777.

(3) Mifflin, A. L.; Konek, C. T.; Geiger, F. M. Tracking Oxytetracycline Mobility Across Environmental Interfaces by Second Harmonic Generation. *J. Phys. Chem. B* **2006**, *110*, 22577-22585.

(4) Salafsky, J. S.; Eisenthal, K. B. Protein Adsorption at Interfaces Detected by Second Harmonic Generation. *J. Phys. Chem. B* **2000**, *104*, 7752-7755.

(5) Felsovalyi, F.; Mangiagalli, P.; Bureau, C.; Kumar, S. K.; Banta, S. Reversibility of the Adsorption of Lysozyme on Silica. *Langmuir* **2011**, *27*, 11873-11882.

(6) Roach, P.; Shirtcliffe, N. J.; Farrar, D.; Perry, C. C. Quantification of Surface-Bound Proteins by Fluorometric Assay: Comparison with Quartz Crystal Microbalance and Amido Black Assay. *J. Phys. Chem. B* **2006**, *110*, 20572-20579.